Available online www.jsaer.com

***Journal of Scientific and Engineering Research*, 2018, 5(1):11-18**

Research Article

ISSN: 2394-2630
CODEN(USA): JSERBR

Inverse Modelling of Turkey-Sivas-Şarkışla Region

Ali Muhittin ALBORA

Istanbul University, Engineering Faculty, Geophysical Department, 34320, Avcilar, Istanbul, Turkey

Abstract As is known one of the most important aspects of the Gravite Prospection is the good analysis of the Bouguer Anomaly Map. The average depth of the geological structure was found by applying the power spectrum method to the Bouguer anomaly map obtained in the Turkey Sivas region-Şarkışla location. The geological structure of that region was modeled by inverse solution method with the help of average depth found. Geological model has been tried to be determined by inversion method of the places forming the anomaly in the region. This method is thought to be a pioneering work in predicting the location of the geological shuttles of petroleum natural gas formations.

Keywords Turkey-Sivas-Şarkışla region, Inverse modelling, Power Spectrum

Introduction

The purpose of the geophysical modeling is to find the parameters of the underground structure causing the anomaly. For this reason, various methods have been developed to find the underground geological structure in the fastest and easiest way possible. According to the idea, the physical properties or geometry of the structure, or both, are tried to be found. They have developed an algorithm for calculating the parameters of geological structures with any shape such as polygonal prism [1; 2]. Backus-Gilbert studied inverse solution approach on gravity profile using inverse solution techniques [3]. Using the recursive inversion technique, they have detected the underground density distribution [4]. For solving the problems in gravitational and seismic prospecting methods, they used Singular Value Segmentation (SDV) [5]. To find the density distribution, Gravite also used the Fourier Transform method [6]. They have studied a program that finds the density difference of two and three dimensional gravity models [7]. They have modeled archaeological sites using the Iterative Cellular Image Processing Algorithm (ICIPA) [8]. Using the Marquart solution technique, they calculated the Gravite and Magnetic inverse solutions of two dimensional polygonal structures [9]. They used Monte Carlo method for inverse solution problems [10]. Using the Streeable Filters technique, they modeled the tectonic lines of the Marmara region [11]. They modeled the dimensions of archeological remains obtained from archaeological sites and creating magnetic effects [12]. They have developed the Forced Neural Networks method, which reveals the parameters of structures with any shape [13; 14; 15]. They have modeled geological structures underground using genetic algorithms [16]. In this study, the Bouguer anomaly map of Şarkışla area of Sivas province was considered and the inverse solution was applied. The average depth of the geological structure is found by applying the AB kesidine two dimensional power spectrum from the Bouguer anomaly map. Based on this average depth, two-dimensional inversion is performed and underground structure is modeled.

Materials and Methods

In geophysics, the inverse solution is interpreted as the calculation of the accepted site model as a group of observed observations. The gravited inversion problem is very resolute. In many solutions, the anomaly observed with the model anomaly found in the inverse solution can be found in very good agreement. However, it is possible to obtain any geological structure not related to the actual mass. The reason for this solvability

comes from two parameters, z_0 (depth) and ρ (density contrast). Therefore, the choice of the parameters of this model is as important as the model of the geophysical structure to be obtained. We can classify the inverse solution method as model parameters and their model response. A model consists of a group relation that shows an observed event with a special mathematical operation. These relies on the number of model parameters we want to calculate true verb. The model response consists of the artificial vertebrae produced from the model. The purpose of the inverse solution is to obtain the model parameters that allow the model response to coincide with the observational data.

Calculation of Gravity Anomalies of Two Dimensional Structures

As you know, gravity is a field of natural potential. In the evaluation of gravity anomalies, the search for the geometric shape of the anomaly creating underground structure forms the basis of modeling studies. We can have information about the geological structure of the ending underground, comparing the theoretical curves with each other, with cross-sections that are measured by land, and structures with any shape. There are many factors to be able to determine the shape of the underground cistern in a good way. The most important factor is the depth. The depth of the object to be modeled is the wavelength of the anomaline that it brings to the field. The anomaly is less affected by the geometry of the deep bodies or the shape changes in deep sections of the cismin. In gravite models, we can treat objects in two and three dimensions. The gravitational field of two-dimensional masses can be calculated from the gravitational fields of three-dimensional masses. We can throw a dimension of three-dimensional masses forever. At this size, the gravitational field remains constant. Thus, the examination of the gravity field of all the mass in the other two dimensions is equivalent to the gravity field of the two-dimensional masses.

$$du = k_0 \, \Delta\rho \frac{dxdydz}{r} \tag{1}$$

Here is k_0 the universal gravitation constant, $\Delta\rho$ density contras and $r^2 = x^2 + y^2 + z^2$ the potential expression of total mass,

$$U = k_0 \Delta\rho \int_x \int_y \int_z \frac{1}{r} dxdydz \tag{2}$$

Moving from here, such a mass is the gravite in the z-axis direction (vertical direction) [17].

$$g_z = \frac{du}{d\,z} = -k_0 \Delta\rho \int_x \int_y \int_z \frac{z}{r^3} dxdydz \tag{3}$$

If we assume that the mass extends infinitely along the y-axis, the formula given by (3) becomes

$$U = 2k_0 \Delta\rho \int_x \int_y \frac{z}{r^2} dxdz \tag{4}$$

Taking advantage of this correlation, the gravitational pull of two-dimensional masses is calculated as follows.

$$g = \frac{\delta\, u}{\delta\, z} = -2k_0 \Delta g \int_x \int_y \frac{z}{r^2} dxdz \tag{5}$$

This equation is a general term used to calculate gravity shots of two-dimensional structures. By taking advantage of this form, gravite shots of structures of any shape can be found. The division of the known geometric shapes to calculate the gravity of two-dimensional structures has been done for a long time. In this way, the gravity anomaly of a vertical dike or prism model can be calculated with known mathematical relationships (Figure 1). A structure or underground topography of any shape can be calculated by dividing the prisms as shown in Figure (2). The sum of each of the prisms that bring this to the fountain gives us gravity shots. The mathematical expression of a vertical prism or dike's gravity attraction is given by (6) [18].

$$g = 2\Delta\rho k_0 \left[\frac{x}{2} \log\left\{ \frac{D^2 + x^2}{d^2 + x^2} \frac{d^2 + (x-b)^2}{D^2 + (x-b)^2} \right\} + \frac{b}{2} \log\left\{ \frac{D^2 + (x-b)^2}{d^2 + (x-b)^2} \right\} - D\left\{ \tan^{-1}\left(\frac{x-b}{D} \right) - \tan^{-1}\left(\frac{x}{D} \right) \right\} + d\left\{ \tan^{-1}\left(\frac{x-b}{d} \right) - \tan^{-1} \frac{x}{d} \right\} \right] \tag{6}$$

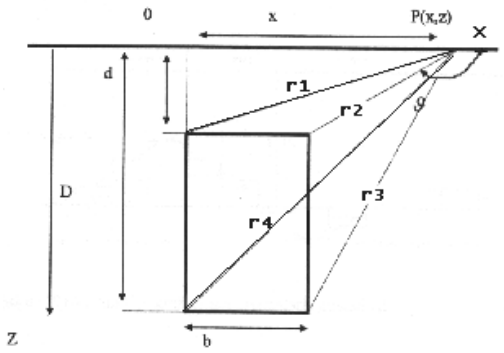

Figure 1: Representation of a gravity anomaly of a prismatic structure.

The underground topography (6) shown in Figure (2) is calculated by prisms using the connection.

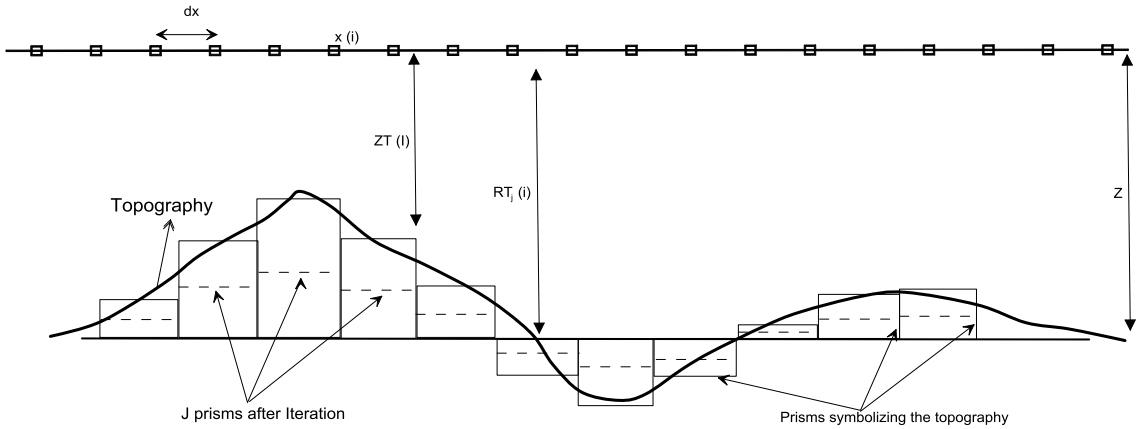

Figure 2: Display of underground topography with prisms.

Here, it is desirable that the topographic structure of the underground intersects the 0 axis of the starting and ending points of the gravity anomaly. If the starting and ending parts of the anomaly intersect near or near zero, it is easier to model the underground topography that causes the anomaly. [19] used the gravity anomaly equation for dike,

$$\Delta g(k) = \sum_{i=2}^{N-1} \left[F_k(z) \right]_{ZT(i)}^{Z} + Ax_k + B, \qquad (7)$$

From here,

$$F_k(z) = 2\Delta\rho k_0 \left\{ z\left[\arctan\left(\frac{(x_k + dx/2)}{z} \right) - \arctan\left(\frac{(x_k - dx/2)}{z} \right) \right] \right.$$

$$\left. + 0.5\left[(x_k + dx/2)\ln\left((x_k + dx/2)^2 + z^2 \right) - (x_k - dx/2)\ln\left((x_k - dx/2)^2 + z^2 \right) \right] \right\} \qquad (8)$$

we get [20].

This correlation shows the k_0 gravity constant, the $\Delta\rho$ density difference, the dx sampling interval, z the average depth of the underground floor topography along the profile. If the average depth of the underground floor topography is known under the first and last points of the anomaly, the depth value is equal to the average depth value (z), otherwise the depth value below the points is taken as zero. Below the average depth $ZT(i) \rangle Z$ is a gravitic effect opposite to the gravitic effect created by a prism extending infinitely in the vertical direction, a prism extending infinitely in the vertical direction above the average depth $ZT\ (i) \langle Z$.

$$[F_k(Z)]_{ZT(i)}^{Z} = -[F_k(Z)]_{Z}^{ZT(i)}$$

The modeling of the underground topography is a repetition of the results that are determined until the calculation of the anomaly with the initial values. Coefficients of regional anomalies A_j and B_j depths to the surface at the end of j repetition $ZT_j(i)$, (I=1,2,3…..n) the theoretical anomaly of such a model,

$$\Delta g_{cal}(k) = \sum_{i=2}^{N-1} [F_K(Z)]_{ZT_j(i)}^{Z} + A_j X_K + B_j \qquad (9)$$

Relation with shown.

At the beginning, the top depth of each prism equals the average depth $(ZT = Z)$ and rate of change of anomaly $\partial F_k(z)/\partial z$, differences in the depths of the prisms from the average depth $Z - ZT_1(i)$ It is assumed that a component equal to,

$$\Delta g(k) = \sum_{i=2}^{N-1} [F_k(z)]_{ZT_j(i)}^{ZT(i)} + dAX_K + dB \qquad (10)$$

be written as. The coefficients of the dA and dB regional anomalies in this connection are the increments of A_j and B_j. If the increments given to the calculated depths, $dZT(i) = ZT_j(i)$ if it is small,

$$[F_k(z)]_{ZT_j(i)}^{ZT(i)} = \left[\frac{\partial F_k(z)}{\partial z}\right]_{ZT_j(i)} .dZT(i) \qquad (11)$$

be written as. Here (2),

$$dg(k) = \sum_{i=2}^{N-1} \left[\frac{\partial F_k(z)}{\partial z}\right]_{ZT_j(i)} dZT(i) + dAX_k + dB \qquad (12)$$

In equation (12), X_k is a known parameter. The relative constants for each anomaly point are computed for the values of dA, dB and dZT (i) through the smallest construction of the error function $\sum df(k)^2$ by applying an appropriate optimization method. When the Marquardt healing method is used,

$$\sum_{k=1}^{N}\sum_{i=1}^{N} \frac{\partial \Delta g(k)}{\partial a_i}\frac{\partial \Delta g(k)}{\partial a_j}(1+\partial\lambda)a_i$$

$$\sum_{k=1}^{N} dg(k)\frac{\partial \Delta g(X_K)}{\partial a_j}, (J = 1,2,.....N) \qquad (13)$$

be written as. In this relation ∂ is the value of, $i = j$ on condition that 1, otherwise $(i \neq j)$ equals 0.

$i = j \;\; \partial = 1$ Here λ Marquardt damping factor.

$a_i = ZT(i+1), \quad i = 1,2,...., N-2$

$a_{N-1} = A$

$a_N = B,$

If the anomalies are taken to be partial derivatives of these parameters,

$$\frac{\partial dg(k)}{\partial a_i} = \left[\frac{\partial F_K(z)}{\partial z}\right]_{ZT(i+1)}, \quad i = 1,2,....N-2$$

$$\frac{\partial dg(k)}{\partial a_{N-1}} = x(k) \quad \text{ve} \quad \frac{\partial dg(k)}{\partial a_N} = 1.0$$

is defined as [21; 22]. Initially, the depths of the top surfaces of the prisms under the entire sampling point are equalized to the average depth. The regional trend coefficients are defined as A=0 and B=0 and the iterative optimization process is established. The anomaly value calculated with such a starting model is zero. For this reason, faults are observed anomalies are added. Repeat operation When the Marquardt damping factor is too large, the error function is completed when an acceptable value is reached or the specified number of iterations is reached.

Power Spectrum

Many methods can be used to obtain the power spectra of two-dimensional data. One of these methods is the Fourier transform method. If we apply Fourier transform to F (x, y) function,

$$V(p,s)=\int_{-\infty}^{\infty}\int_{-\infty}^{\infty} F(x,y)\exp(-2\pi i(px+sy))\,dx\,dy \qquad (14)$$

Where p and s represent the waveguide in the direction of the x and y axes, respectively. In general, V (p, s) is a complex size. R is to show the real part of these complex quantities as the IQ image part;

$$V(p,s)=R+IQ \qquad (15)$$

We will mark for each p and s frequency bands as we know, the values of $(R^2+Q^2)^{1/2}$ give the power spectrum of the field F (x, y).

Many researchers to calculate Gravite and Magnetic anomalies have used this method. Some of these researchers [23; 24; 25; 26; 27; 28].

Geology of the Region

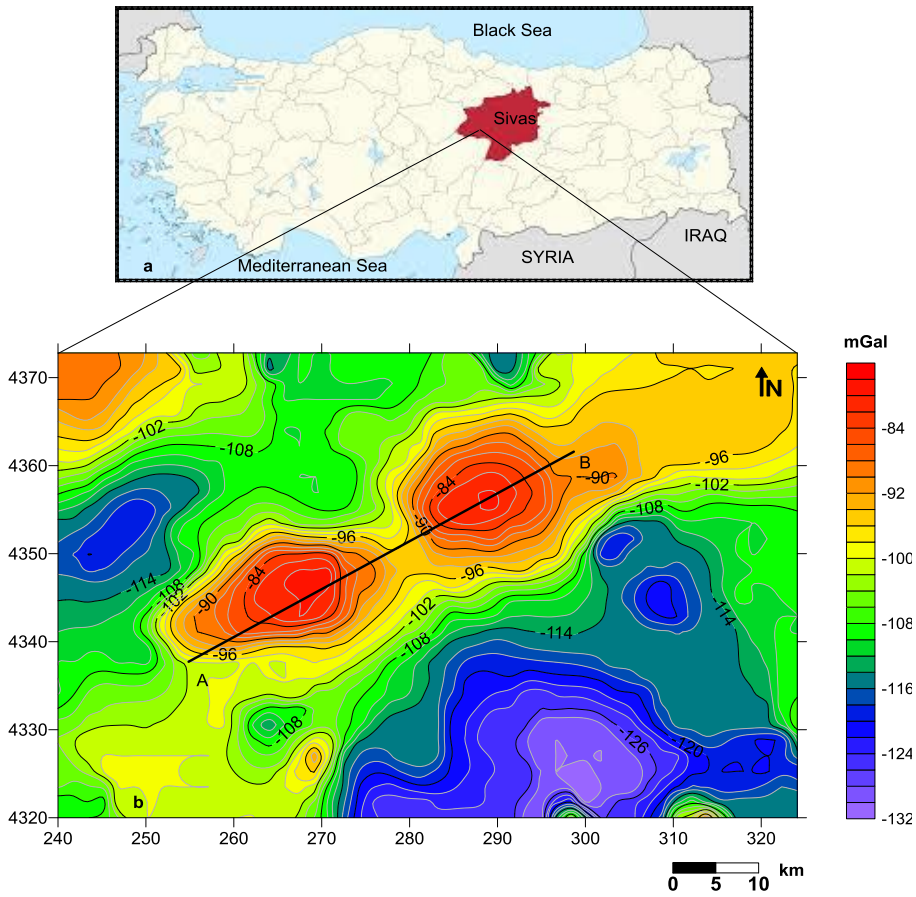

Figure 3: Turkey-Sivas-Şarkışla a- location map b- Bouguer anomaly map and AB section.

There are two distinct tectonic cycles, the Old Tectonic Period and the New Tectonic Period. The old tectonic period is represented by continued geological events and constructions until the end of Young Miocene. These are the compressional stresses affecting the region at the end of the Paleocene, Eocene and Oligocene, and the developed NE-SW trending folds and bindings. In addition, NW-SE trending strike-slip faults have also developed. Pliocene aged terrestrial sediments and their age-related vertical movements represent the new tectonic period. Upper Cretaceous-Paleocene formations reach 3000 m in thickness. Conglomerates and clayey limestones reaching a thickness of 1400 meter represent the Eocene. The Oligocene aged units consist of lagoonal gypsum and terrestrial sediments of a total thickness of 3200 meter. Pliocene is represented by 650 meter thick conglomerates and basalts, while Quaternary is represented by aliions [29].

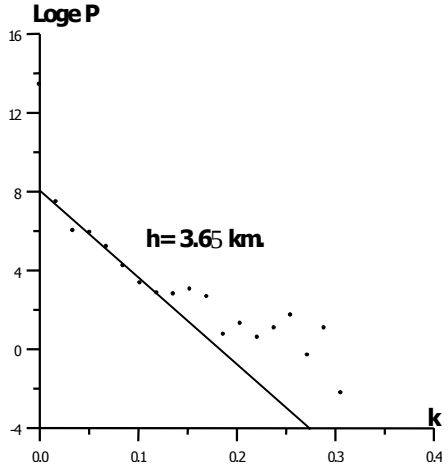

Figure 4: Power spectrum of AB cross section from bouguer anomaly map.

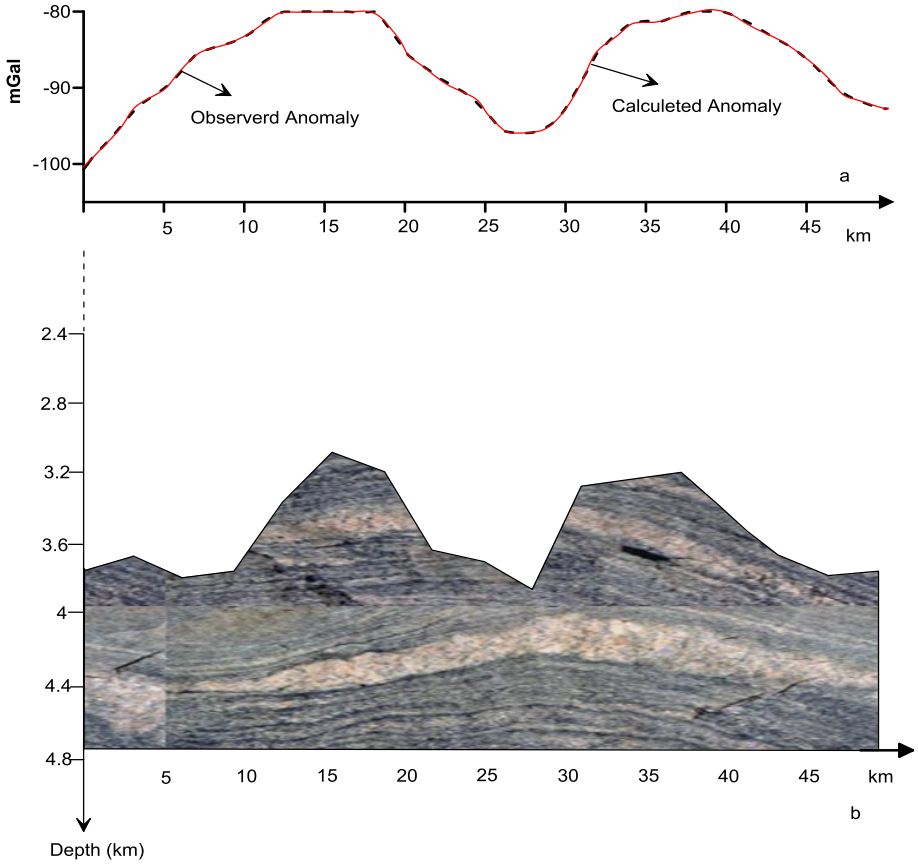

Figure 5: Measured and calculated anomaly section taken from Sivas-Şarkışla region a) Bouguer anomaly map b) Geological model obtained as inverse solution result.

Conclusion and Discussion

The Sivas-Şarkışla region in Turkey was studied in the field study (Figure 3a). AB section was taken from the Bouguer anomaly map of the Turkish Petroleum Corporation (TPAO) in the region (Figure 3b). The Power Spectrum was applied to the Bouguer anomaly map and the mean depth of the region was 3.65 km. (Figure 4). The calculated average depth information is used as the input value in the inversion process. Using the geological information, the density difference of the environment was taken as approximately 1 gr / cm3. Inverse solution process was applied by using the AB section (Figure 5a) and average depth value obtained from the Bouguer anomaly map. A perfect overlap was achieved as a result of the second round of the inverse solution. As a result of the inverse solution, the underground structure is modeled as given in Figure 5b. When the obtained model structure and geological structure of the region are examined, it is observed that there is a good fit.

Contributions

We thank Turkish Petroleum Cooperation (TPAO) and for their gravity data.

References

[1]. Talwani, M., & Ewing, M., (1960). Rapid computation of gravitational attraction of 3D bodies of arbitrary shape. *Geophysics*, 25; 203-225.

[2]. Talwani, M., (1965). Computation with the help of a digital computer of magnetic anomalies caused by bodies of arbitrary shape. *Geophysics*, 30; 797-817.

[3]. Green, W. R., (1975). Inversion of gravity profiles by use of a Backus-Gilbert approach. *Geophysıcs*, 45; 403-419.

[4]. Last, B. J., & Kubik, K., (1983). Compact Gravity Inversion. *Geophysıcs,* 48; 713-721.

[5]. Lines, L. R., & Treitel, S., (1984). Tutorial a Review of Least-Squares Inversion and ıts Application to Geophysical Problems. *Geophysical Prospecting*, 32; 159-186.

[6]. Mareschal, J. C., 81985). Inversion of potential field data in Fourier transform domain. *Geophysics*, 50; 685-691.

[7]. Murthy, I. V. R., & Krishnamacharyulu, S. K. G., (1990). Automatıc inversion of gravity anomalies of faults. *Computers & Geosciences*, 16; 539-548.

[8]. Osman, O., Uçan. O. N., & Albora, A. M**.,** (2002). Evaluation of Hittite Archaeological Ruins Using Iterative Cellular Image Processing Algorithm (Icipa). *The 2rd International Conference on Earth Sciences and Electronics (ICESE-2002)*. V 2, 219-227.

[9]. Murthy, I. V. R., & Rao, P. R., (1993). Inversion of Gravity and Magnetic anomalies of two-dimensional polygonal cross sections. *Computers & Geosciences*, 19; 1213-1228.

[10]. Mosegaard, K., & Tarantola, A., (1995). Monte Carlo sampling of solutions to inverse problems. *Journal of Geophysics Research*, 100; 12431-12447.

[11]. Albora A.M., (2013). A View of Tectonic Stucture of Marmara Regıon (NW Turkey) Using Streeable Filters. *American Geophysical Union (AGU), ABD*, pp.1-2.

[12]. Albora, A. M., Hisarlı, Z. M., & Uçan, O. N. (2004). Application of Wavelet Transform to Magnetic Data Due to Ruins of Hittite Civilization in Turkey. *Pure and Applied Geophysics*, 161; 907-930.

[13]. Osman, O., Albora, A. M., & Ucan, O. N., (2006). A new approach for resıdual gravity Anomaly profile ınterpretatıons: Forced neural network (FNN). *Annals of Geophysıcs*, 49 (6);1201-1208.

[14]. Osman, O., Albora, A. M., & Ucan, O. N., (2007). Forward modeling with Forced Neural Networks for gravity anomaly Profile. *Mathematical Geology*, 39:593-605.

[15]. Albora, A. M., & Osman, O., (2016). Modeling of Turkey-Manyas region using Forced Neural Networks. *Journal of Scientific and Engineering Research* , 3, 567-573.

[16]. Osman, O., & Albora, A. M., (2015). Modeling of Gravity Anomalies due to 2D Geological Structures using Genetic Algorithm. *IU-Journal of Electrical & Electronics Engineering*, 15(2), 1929-1935.

[17]. Bhaskara, R., Prakash, M. J. & Ramesh, B. N., (1990). 3D and 2.5D modeling of gravity anomalies with variable density contrast. *Geophysical Prospecting*, 38, 411-422.

[18]. Telford, W. M., Geldart, L. P., Sheriff, R. E., & Keys, D. A., (1980). Applied Geophysics. *Cambridge University Preess*, Cambridge.
[19]. Rao, B. S. R., & Murthy, I. V. R. (1978). Gravity and magnetic methods of prospecting: Arnold-Heinemann (India) Pvt. Ltd., AB/9 Safdar jang Enclave, New Delhi, 390.
[20]. Murthy, I. V. R. & Rao, S. J., (1989). A Fotran 77 Program for Inverting Gravity Anomalies of Two-Dimensional Basement Structures. *Computers & Geosciences*, 15, 1149-1156.
[21]. Sarı, C., Şalk, M., Çifçi, G., & Vural, T., (1997). Yeraltı taban topoğrafyasının iki boyutlu Gravite-Manyetik ters çözüm yöntemiyle saptanması ve Ankara-Polatlı bölgesine uygulanması. *Jeofizik*, 11, 21-33 (Turkish paper).
[22]. Albora, A. M., (1998). Hatay bölgesi gravite yoğunluk dağılımının araştırılması. *İstanbul Üniversity, Institute of Science and Technology*, PhD thesis, 119 pp.
[23]. Bhattacharya, B. K., (1966). Continuous Spectrum of the Total-Magnetic-Field Anomaly Due to a Rectangular Prismatic Body. *Geophysics*, 31(1), 97-121.
[24]. Spector, A., & Grant, F. S., (1970). Statistical Models for Interpreting Aeromagnetic Data. *Geophysics*, 35(2), 293-302.
[25]. Hahn, A., Kind, E. G., & Mishra, D. C., (1976). Depth Estimation of Magnetic Sources by Means of Fourier Amplitude Spectra. *Geophysical Prospecting*, 24, 287-308.
[26]. Cianciara, B., & Marcak, H., (1976). Interpretation of Gravitv Anomalies by Means of Local Power Spectra. *Geophysical Prospecting*, 24, 273-286.
[27]. Akçığ, Z., & Pınar, R., (1990). Gravite Verilerine Güç Spektrumu Yönteminin Kayan Pencereli Uygulaması. *Jeofizik*, 4(1), 37-40 (Turkish paper).
[28]. Akgün, M., Akçığ, Z., & Pınar, R., (1994). Gravite Yönteminde Güç Spektrumunun Değişik Modellere Uygulanması. *Jeofizik*, 8(1), 63-69 (Turkish paper).
[29]. Gökten, E., (1984). Şarkışla (Sivas) güney-güneydoğusunun stratigrafisi ve jeolojik evrimi. *Türkiye Jeoloji Kurumu Bülteni*, 26,167-176 (Turkish paper).